Structures of the Cuprous-Thiolate Clusters of the Mac1 and Ace1 Transcriptional Activators

Kenneth R. Brown,[‡] Greg L. Keller,[‡] Ingrid J. Pickering,[§] Hugh H. Harris,[§] Graham N. George,*[,§] and Dennis R. Winge*[,‡]

University of Utah Health Sciences Center, 50 N. Medical Drive, 4C312, Salt Lake City, Utah 84132, and Stanford Synchrotron Radiation Laboratory, Stanford Linear Accelerator Center, Mississippi 69, 2575 Sand Hill Road, Menlo Park, California 94205

Received December 18, 2001; Revised Manuscript Received March 20, 2002

ABSTRACT: X-ray absorption spectroscopy on the minimal copper-regulatory domains of the two copper-regulated transcription factors (Ace1 and Mac1) in *Saccharomyces cerevisiae* revealed the presence of a remarkably similar polycopper cluster in both proteins. The Cu-regulatory switch motif of Mac1 consisting of the C-terminal first Cys-rich motif, designated the C1 domain, binds four Cu(I) ions as does the Cu-regulatory domain of Ace1. The four Cu(I) ions are bound to each molecule in trigonal geometry. An extended X-ray absorption fine structure (EXAFS) arising from outer-shell Cu···Cu interactions at 2.7 and 2.9 Å was apparent in each Cu(I) complex indicative of a polycopper cluster. The intensity of the 2.9 Å Cu···Cu backscatter peak, apparently diminished by partial cancellation, dominates the EXAFS. The results suggest that CuAce1 and CuMac1(C1) contain somewhat distorted forms of a known $[Cu_4-S_6]$ cage in which a core of Cu atoms forming an approximate tetrahedron is bound by bridging thiolates above each of the six edges. The tetracopper clusters bound by Ace1 and Mac1 differ in that the Ace1 cluster is coordinated entirely by cysteinyl thiolate, whereas the cysteine-deficient Mac1 cluster appears to consist of a $Cu_4(S-Cys)_5(N-His)$ cluster with a bridging histidyl-derived nitrogen.

Saccharomyces cerevisiae contains two copper-regulated transcriptional activators, Ace1 and Mac1 (*1*). These factors activate expression of genes whose products maintain copper homeostasis. Ace1 and Mac1 are nuclear factors whose activity is coupled to the copper status of yeast cells. Cu-activation of Ace1 occurs through formation of a tetracopper thiolate cluster in one of two DNA binding domains. Cu(I) binding to Ace1 induces a conformation that enables Ace1 to bind to its cognate DNA binding site. In contrast, Cu(I) binding to Mac1 inhibits its function as a transcriptional activator. Copper metalloregulation of Ace1 and Mac1 is at the core of yeast copper homeostasis. We show in this report that Cu(I) binds to both factors in similar polycopper clusters.

Mac1 activates the expression of six genes, three of which function in copper ion uptake across the plasma membrane; the function of the other three is unknown. Two Cu ion uptake genes encode cell surface copper ion permeases, Ctr1 and Ctr3 (*2*, *3*). The third gene encodes the Fre1 metalloreductase that functions in reductive mobilization of copper ions (*1*, *4*, *5*). Mac1 activates expression of these three genes in Cu-deficient cells, resulting in increased effectiveness in acquiring Cu ions from the growth medium. As cells become replete for copper ions, Mac1 is specifically inhibited. The mechanism of Cu-inhibition of Mac1 function appears to arise through Cu(I) binding to Mac1.

Mac1 is a typical fungal transcriptional activator protein with two separate functional domains, an N-terminal DNA binding domain and a C-terminal transactivator. The minimal DNA binding domain maps to the N-terminal 159 residues, which bind two Zn(II) ions (*6*). The transactivator motif in Mac1 lies within two repeated C-terminal Cys-rich motifs with a Cys-x-Cys-x_4-Cys-x-Cys-x_2-Cys-x_2-His consensus sequence (*11*, *12*). Cu-inhibition of Mac1 function involves both Cu-dependent loss of in vivo DNA binding activity (*2*) and Cu-dependent inhibition of transactivation function (*5*, *11*). Cu-dependent abrogation of DNA binding by the N-terminal DNA binding domains requires C-terminal sequences (*6*). Likewise, Cu-modulation of transactivation activity requires both the C-terminal transactivation domains and a portion of the N-terminal DNA binding domain (*11*). The prediction is that the repressed conformation of Mac1 is an intramolecular complex involving both the N-terminal and C-terminal domains. Cu(I) binding to the C-terminal Cys-rich motifs induces an intramolecular interaction with the N-terminal DNA binding domain (*13*). The intramolecular interaction appears to inhibit both DNA binding and transactivation.

The two carboxyl-terminal Cys-rich repeats in Mac1, designated C1 and C2, bind a total of eight Cu(I) ions (*13*). A series of mutations within the C1 motif consisting of residues 264−279 abrogate Cu-regulation of Mac1 (*3*, *12*, *14*). All but one of the constitutive Mac1 mutations occur in one of the conserved six residues in the C_{264}-x-C-x_4-C-

[†] This work was supported in part by Grant ES 03817 from the National Institutes of Environmental Health Sciences, NIH, to D.R.W. K.R.B. was supported by a T32 training grant (DK07115) from the National Institutes of Health. SSRL is funded by the Department of Energy, Offices of Basic Energy Sciences and Biological and Environmental Research, and the National Institutes of Health, National Center for Research Resources, Biomedical Technology Program.

* To whom correspondence should be addressed.

[‡] University of Utah Health Sciences Center.

[§] Stanford Synchrotron Radiation Laboratory.

10.1021/bi0160664 CCC: $22.00
Published on Web 04/24/2002

x-C-x_2-C-x_2-H_{279} C1 motif (*3*, *12*, *14*). Engineered mutations in the second Cys-rich C2 motif did not yield a constitutively active Mac1. These results are consistent with the C1 motif being the major Cu-regulatory switch. The two Cys-rich motifs appear to function independently: the C1 Cys-rich motif appears to be a functional copper-regulatory domain, whereas the C2 motif is the major transactivator.

Exposure of yeast cells to elevated copper (≥ 1 μM) triggers the activation of Ace1 within the nucleus and the subsequent transcriptional activation of three genes whose products protect the cell from the potential cytotoxicity of Cu ions. The Cu-activated genes include the *CUP1* and *CRS5* metallothioneins and *SOD1* superoxide dismutase (*15*−*19*). *CUP1* is the dominant locus that confers the ability of yeast cells to propagate in media containing copper salts (*18*, *20*, *21*). The Cup1 metallothionein binds seven Cu(I) ions within a buried polycopper thiolate cluster that effectively buffers the cytosolic copper levels to maintain a low reactive pool of Cu(I) (*23*−*25*). The second type of metallothionein in yeast, Crs5, is also copper metalloregulated in its expression (*17*).

Ace1 also has separate DNA binding and transactivation domains. The DNA binding segment of Ace1 consists of two domains, a 40-residue Zn module (seen also in the Mac1 DNA binding domain) and a 60−70 residue Cu-regulatory domain (*26*, *27*). The tetracopper domain contains eight essential cysteines present as four Cys-$x_{1,2}$-Cys sequence motifs (*27*). Cu-activation of Ace1 involves formation of a tetracopper cluster within the Cu-regulatory domain. Cu(I) binding stabilizes a conformation that exhibits specific and high affinity DNA binding. Luminescence and X-ray absorption spectroscopy of the CuAce1 and its ortholog in *Candida glabrata* CuAmt1 showed that the bound Cu ions are present as Cu(I) (*27*). The existence of a polycopper cluster was inferred from a prominent outer-shell X-ray scatter peak at 2.7 Å (*27*, *28*). The extended X-ray absorption fine structure (EXAFS) of this feature gave an acceptable fit only by the inclusion of a heavy scatterer atom indicating a polycopper cluster. EXAFS of the crystallographically defined tetracopper thiolate cluster $[Cu_4(SPh)_6]^{2-}$ revealed a spectrum similar to that of CuAce1 (*29*).

In this study, the Cu-bound structures of Ace1 and Mac1 were compared by X-ray absorption spectroscopy. The Cu(I) ions bound to the C1 motif in Mac1 are present in a polycopper cluster that exhibits properties similar to those of the tetracopper cluster in Ace1. Thus, both Cu-sensing nuclear transcription regulators in yeast contain polycopper thiolate clusters. Polycopper clusters may be conserved structural motifs in Cu-regulatory proteins in other species.

MATERIALS AND METHODS

Purification of Mac1 Truncates. GI698 cells were transformed with one of two pTrxFus vectors (InVitrogen) containing a thioredoxin-*MAC1* fusion gene cloned in as a *Kpn*1/*Xba*1 fragment. Two fusion molecules were engineered consisting of thioredoxin fused to two segments of Mac1 at the C-terminal end. One construct consisted of Mac1 residues 254−307 (C1 motif), and the other consisted of Mac1 residues 254−346 (C1,C2 motifs). Transformants were induced with tryptophan (100 μg/mL) at $OD_{600\ nm} = 0.6$, and 1.5 mM $CuSO_4$ was added. Cells were harvested by centrifugation 3 h after induction. Two buffers, buffer A (20 mM Tris pH 8.0 with 4 mM DTT) and buffer B (buffer A with 0.75 M NaCl), were used in the purification. Frozen cells (2−4 L) were thawed in 45 mL of buffer A and sonicated. The lysate was clarified by centrifugation at 200 000 g for 35 min, and the supernatant was loaded onto a Pharmacia DEAE HiPrep 16/10 column equilibrated in buffer A. The protein was eluted over a 20 bed volume gradient to 80% buffer B. The protein was concentrated and loaded onto a Pharmacia Superdex G-75 26/60 equilibrated in 10 mM TrisCl, pH 8.0, 4 mM DTT, and 150 mM NaCl. Thioredoxin−Mac1-containing fractions were identified by their mass and copper content using SDS-polyacrylamide gel electrophoresis and atomic absorption spectroscopy, respectively.

Purification of Ace1 Truncates. A series of vectors were generated for the expression of Ace1 truncates consisting of the Cu-regulatory *ACE1* domain (residues 40−100) and varying amounts of the GRP minor groove motif. Each truncated gene was generated with optimal *Escherichia coli* codons and subcloned into pET9A as an *Nde*1/*Bam*H1 fragment. BL21 (DE3, pLysS) cells were transformed with the vectors to yield expression of Ace1 truncates of residues 36−100, 38−100, and 40−100. Cells were cultured at 37 °C in LB broth with kanimycin to $OD_{600\ nm} = 0.6$ and induced with 0.4 mM IPTG for 3 h. $CuSO_4$ was added 30 min after IPTG induction to a final concentration of 1.4 mM. Cells were harvested by centrifugation, washed in 0.25 M sucrose, and frozen. Cells were thawed in 45 mL of buffer C (10 mM $NaPO_4$, 5 mM NaCitrate pH 7.5) and sonicated. Protamine sulfate was added to the clarified lysate to a final concentration of 2.5 mg/mL. Protamine sulfate precipitation is required as Ace1 forms nonspecific DNA complexes with sheared bacterial DNA. The clarified supernatant was loaded onto a Pharmacia CM-HiPrep 16/10 equilibrated in buffer C. The protein was eluted with a linear gradient from 0 to 0.75 M KCl. Ace1 fractions were identified by Cu(I) luminescence at 575 nm and quantitation of copper by atomic absorption spectroscopy. Ace1-containing fractions were diluted and loaded on a Pharmacia MonoS 5/5 column equilibrated in buffer C. The protein was eluted with a linear gradient of 0−0.75 M KCl. SDS-Polyacrylamide gel electrophoresis was carried out to assess the purity of the Ace1 elution fractions.

DNA Binding Assay. Oligonucleotides spanning the CuAce1 responsive element (CuRE) in *CUP1* were synthesized with an ABI 380B DNA synthesizer. The oligonucleotides and gel shift conditions were described previously (*29*). The protein/DNA incubations included 0.01% Nonidet P40, 30 μg/mL poly (dI-dC), 65 mM KCl, 10 mM canine albumin, 0.25 mM $MgCl_2$, 4 mM DTT, and 0.5 μg of protein.

Assays. The copper concentration of the protein samples was measured using a Perkin-Elmer (AAnalyst 100) atomic absorption spectrophotometer. Protein was quantified by amino acid analysis after hydrolysis in 5.7 N HCl at 110 °C in vacuo. A Beckman 6300 analyzer was used for the analyses. Optical absorption spectroscopy was carried out on a Beckman DU640 apparatus. Luminescence was measured on a Perkin-Elmer 650-10S fluorimeter with excitation set at 300 nm.

X-ray Absorption Spectroscopy. X-ray absorption spectroscopy was carried out at the Stanford Synchrotron

Radiation Laboratory with the SPEAR storage ring operating at 3.0 GeV and containing between 60 and 100 mA. Data were collected on beamlines 9−3 and 7−3, employing wiggler fields of 2 and 1.8 T, respectively. In both cases, a Si(220) double-crystal monochromator was employed. Beamline 9−3 is equipped with a Rh-coated vertically collimating mirror upstream of the monochromator and a bent-cylindrical Rh-coated focusing mirror downstream of the monochromator; harmonic rejection was accomplished by adjusting the cutoff energy of the mirrors to 12 keV. Beamline 7−3 contains no mirrors, and in this case harmonic rejection was accomplished by detuning one monochromator crystal to approximately 50% off peak, while energy resolution was optimized by using a monochromator vertical entrance aperture of 1 mm. Incident X-ray intensity was monitored using nitrogen-filled ionization chambers, and X-ray absorption was measured as the X-ray Cu Kα fluorescence excitation using germanium array detectors (30 elements on beamline 9−3, and 13 on 7−3). During data collection, samples were maintained at a temperature of approximately 10 K, using an Oxford Instruments liquid helium flow cryostat. From three to eight 30 min scans were accumulated, and the absorption of a copper metal foil was measured simultaneously by transmittance. The energy scale was calibrated with reference to the lowest energy inflection point of the copper foil, which was assumed to be 8980.3 eV. EXAFS spectroscopy data analysis was done using the EXAFSPAK software (http://ssrl.slac.stanford.edu/exafspak.html), and the phase and amplitude functions were calculated using the ab initio code FEFF version 8.2 (*30*, *31*). Data from two synthetic copper model compounds were used, a trigonal $[Cu_4(SPh)_6]^{2-}$ cluster (*32*) and a digonal $[Cu(SC_{10}H_{12})_2]^{2-}$ compound (*33*).

Density Functional Calculations. Optimized geometries for $[Cu_4(SH)_6]^{2-}$ and $[Cu_4(methylimidazolyl)(SH)_5]^{2-}$ were determined using the program $Dmol^3$ Materials Studio version 2.0 (*34*, *35*). The Becke exchange (*36*) and Perdew correlation (*37*) functionals were used in all cases to calculate both the potential during the SCF and the energy. Double numerical basis sets included polarization functions for all atoms. Calculations were spin-unrestricted, and effective core potentials were used in place of Cu core orbitals ($n = 1, 2$). No symmetry constraints were applied. Optimization energy tolerances of 2.0×10^{-5} Ha were used, but no vibrational analysis was performed. Density Functional Theory (DFT) is expedient for transition metal clusters of this size and has been extensively validated (*38*−*42*). Starting geometries were based on the X-ray crystal structure coordinates of $[Cu_4(SPh)_6]^{2-}$ (*32*), by replacing phenyl groups with hydrogens (to speed up the calculation) and by replacement of one thiolate by methylimidazole that was used to model a histidine ligand.

RESULTS

Purification of Cu-Regulatory Domain of Mac1. We previously demonstrated that intact Mac1 binds eight Cu(I) ions per molecule and the Cu content was halved in a construct with a mutation in the C-terminal C1 motif (*13*). To verify that the Cu(I) binding occurred in the C1/C2 motifs, two thioredoxin/Mac1 fusion genes were constructed for expression of either the C1 or C1/C2 motifs fused to thioredoxin. The resulting fusions consisted of Mac1 C1 residues (254−307) or Mac1 C1/C2 residues (254−346) fused to N-terminal thioredoxin. Purification of thioredoxin-C1 and thioredoxin-C1/C2 was accomplished by conventional chromatography. The fusion proteins as isolated exhibited a single band on polyacrylamide gel electrophoresis stained with Coomassie blue. The thioredoxin-C1 protein as isolated bound 4.2 ± 0.3 (six independent isolates) mol equiv of Cu per molecule. The thioredoxin-C1/C2 fusion bound 7.5 (one isolate) mol equiv of Cu per molecule, which is consistent with our previous report of 8 mol equiv of Cu ions bound to intact Mac1 (*13*). The observed Cu binding stoichiometry of 4 mol equiv for the C1 motif is consistent with four Cu ions bound to each of the two Cys-rich sequence motifs. The C1 motif has no activity other than Cu(I) ion binding that can be measured to assess the structural integrity of the motif.

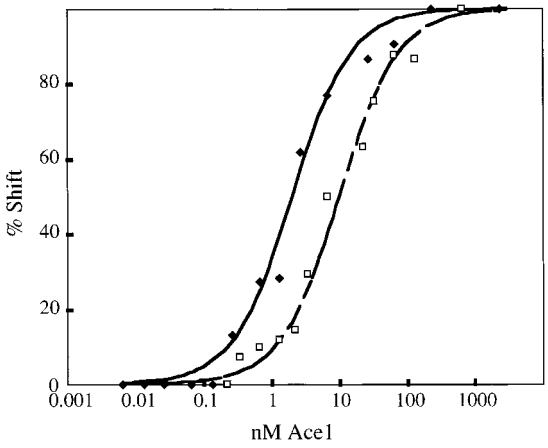

FIGURE 1: DNA binding by two variants of the Ace1 copper-regulatory domain. Interaction of CuAce1 consisting of the minimal Cu-regulatory domain with an appended RGRP motif (residues 36−100) for a DNA duplex containing the CuRE sequence is compared to that of a construct with only RP appended to the minimal Cu-regulatory domain (residues 38−100). DNA binding was assessed by the electrophoretic mobility shift assay.

Purification of Cu-Regulatory Domain of Ace1. One goal was to compare the Cu(I) complex of Mac1 to the Cu(I) complex of Ace1. The minimal Cu-regulatory domain of Ace1 consists of residues 40−100. This domain expressed in bacteria bound four Cu(I) ions but failed to bind a *CUP1* CuRE DNA oligonucleotide. Various Ace1 constructs were engineered with different segments of the N-terminal Zn domain fused to the minimal Cu-regulatory domain. The addition of just the RGRP minor groove binding motif to the minimal Cu-regulatory domain (residues 40−100) restored DNA binding. This minimal CuAce1 (residues 36−100) complex bound 4.0 ± 0.5 (15 isolates) Cu(I) ions per molecule. The purified CuAce1 complex bound a DNA oligonucleotide containing a *CUP1* CuRE with a binding affinity of 2 nM (Figure 1). The addition of only an RP dipeptide on the Cu-regulatory domain yielded specific DNA binding but with an affinity reduced to 10 nM. All spectroscopic studies were carried out on the DNA binding Ace1 truncate (residues 36−100).

Spectroscopy of the Cu(I) Complexes. The Cu(I) complexes of Ace1 and Mac1 show transitions in the ultraviolet range consistent with thiolate coordination. The transitions

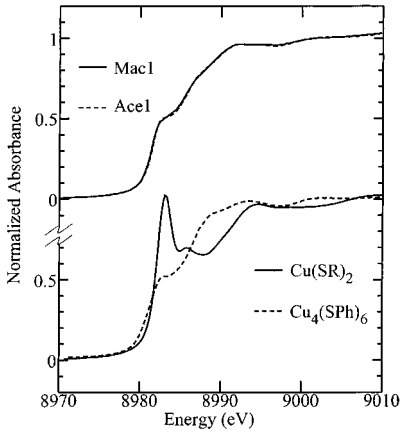

FIGURE 2: Comparison of the copper K X-ray absorption near-edge spectra of Mac1, Ace1, the trigonally coordinated $[Cu_4(SPh)_6]^{2-}$, and the digonally coordinated $[Cu(SC_{10}H_{12})_2]^{2-}$.

are bleached by acidification. The CuAce1 complex is luminescent with emission shifted to 580 nm. In contrast, the CuMac1(C1) complex is weakly luminescent, consistent with greater solvent quenching in the CuMac1(C1) complex (data not shown).

To structurally characterize the metal sites, X-ray absorption spectroscopy was carried out on CuAce1 and CuMac1(C1). The Cu K near-edge spectra of CuAce1 and CuMac1(C1) were very similar (Figure 2). Cuprous compounds have characteristic near-edge spectra that can be used as an indicator of geometry. For digonally coordinated Cu(I) with linear geometry the degenerate $4p_{x,y}$ orbitals are nonbonding and retain pure p character, leading to an intense dipole-allowed ($\Delta l = \pm 1$) 1s→4p transition at around 8983 eV in the near-edge spectrum (*33*, *43*). For trigonally coordinated Cu(I), the degeneracy is lifted and s−p mixing occurs, leading to a reduction in dipole-allowed intensity of the 8983 eV peak (*43*). Figure 2 also compares the protein near-edge spectra with those from two cuprous thiolate complexes, the trigonal $[Cu_4(SPh)_6]^{2-}$ and the digonal $[Cu(SC_{10}H_{12})_2]^{2-}$ (*29*, *44*). It can be seen that the protein spectra closely resemble the spectrum of the trigonal and not the digonal species.

The EXAFS spectra and corresponding Fourier transforms of CuAce1 and CuMac1 are very similar (Figure 3), and analysis of the EXAFS by curve-fitting also indicates that the structure of the Cu(I) sites in these two proteins are quantitatively related (Table 1). The Fourier transforms for both proteins (Figure 3) are dominated by strong backscattering from Cu−S at around 2.25 Å, with a smaller contribution from Cu···Cu backscattering at around 2.7 Å. Curve-fitting analysis of the CuAce1 EXAFS using a simple two-shell model indicated three Cu−S interactions at 2.25 Å (in agreement with the near-edge spectra shown in Figure 2) and a single Cu···Cu interaction. The Cu···Cu coordination number of one is lower than the value of three obtained for a synthetic tetranuclear cluster (*29*). However, when two different Cu···Cu interactions were included, a better fit was obtained with coordination numbers of 2 and 1 at 2.7 and 2.9 Å, respectively (Table 1). These Cu···Cu EXAFS are substantially out of phase (Figure 4), effectively reducing the intensity of the 2.7 Å interaction by one due to cancellation with the 2.9 Å interaction. This analysis is in agreement with the copper stoichiometry of four per peptide. A similar fit was obtained for the CuMac1(C1) data, although

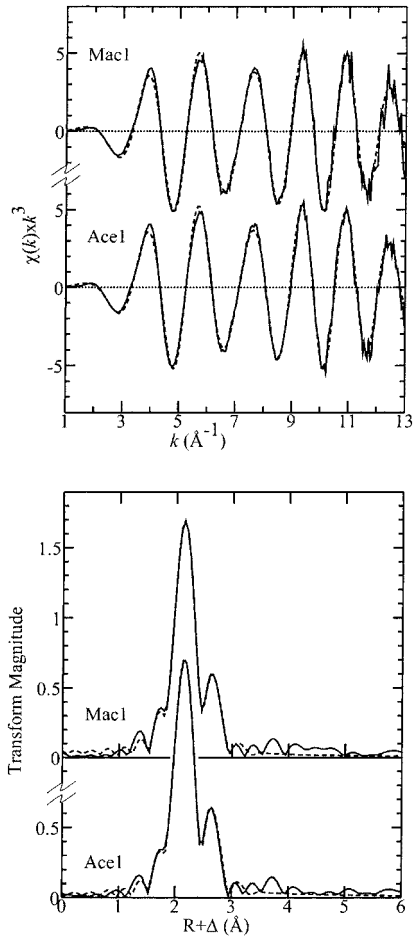

FIGURE 3: EXAFS oscillations (upper panel) and EXAFS Fourier transforms (lower panel) of CuMac1 and CuAce1. Solid lines indicate experimental data and the broken lines the best fits obtained with the parameters given in Table 1. All Fourier transforms are phase-corrected for Cu−S backscattering.

the improvement in the fit with two vs one type of Cu···Cu interaction is less pronounced, due to the relatively higher noise content of this data set (Table 1). These results suggest that CuAce1 and CuMac1(C1) contain somewhat distorted tetranuclear clusters, similar to those previously reported for low-molecular weight $[Cu_4(SR)_6]^{2-}$ species (*32*), in which an approximately tetrahedral core of Cu atoms is bound by bridging thiolates above each of the six edges. A variety of subtle distortions from purely tetrahedrally arranged copper ions are observed in low-molecular weight $[Cu_4(SR)_6]^{2-}$ species (*32*). Our results suggest that similar but slightly larger distortions are present in CuAce1 and CuMac1, presumably imposed by the protein conformation. These distortions need not be large; for example, an increase in two opposite Cu−S−Cu angles of only 6° would result in the Cu···Cu vectors derived from the curve-fitting.

Figure 5 shows the effects of binding to DNA on the EXAFS of the Ace1 metal cluster. The Cu−S intensity is essentially unchanged, but the Cu···Cu intensity is much diminished. Although this decrease in Cu···Cu intensity can be modeled in several different ways, three inequivalent Cu···Cu distances, with partial cancellation in each, gave the best fit that is shown in Figure 5. An example of a symmetrical (and again slight) cluster distortion that might result in this distribution of Cu···Cu vectors is twisting of the tetrahedron about an axis normal to two Cu···Cu vectors.

Table 1: Results of EXAFS Curve Fitting of CuAce1 and CuMac1(C1)[a]

sample	interaction	N	R (Å)	σ^2 (Å^2)	ΔE_0 (eV)	error
CuAce1	Cu−S	3	2.247(1)	0.0044(1)	−18.0(8)	0.140
	Cu···Cu	1	2.695(2)	0.0066(2)		
CuAce1	Cu−S	3	2.251(1)	0.0043(1)	−16.9(7)	0.115
	Cu···Cu	2	2.704(2)	0.0086(2)		
	Cu···Cu	1	2.902(6)	0.0088(2)		
CuMac1	Cu−S	3	2.247(1)	0.0043(1)	−17.9(6)	0.228
	Cu···Cu	1	2.697(4)	0.0071(4)		
CuMac1	Cu−S	3	2.251(2)	0.0043(1)	−16.9(5)	0.211
	Cu···Cu	2	2.705(4)	0.0088(4)		
	Cu···Cu	1	2.891(9)	0.0089(4)		
CuMac1	Cu−S	2.5	2.255(3)	0.0031(2)	−16.8(8)	0.210
	Cu−N	0.5	2.002(18)	0.0030(2)		
	Cu···Cu	2	2.703(5)	0.0088(4)		
	Cu···Cu	1	2.891(9)	0.0089(4)		
CuAce1/DNA	Cu−S	3	2.250(1)	0.0049(1)	−16.6(9)	0.164
	Cu···Cu	1	2.675(5)	0.0089(6)		
	Cu···Cu	1	2.752(7)	0.0092(6)		
	Cu···Cu	1	2.913(8)	0.0096(7)		

[a] For CuAce1, fits are shown for two scenarios, a single vs two Cu···Cu distances. For CuMac1(C1), fits are shown for the same two Cu···Cu distance scenarios, and in addition, all thiolate coordination vs thiolate coordination with a single His imidazole. Coordination numbers are listed as N and interatomic distances R are given in Å, Debye−Waller factors σ^2 (the mean-square deviations in interatomic distance) in Å^2, and threshold energy shifts ΔE_0 in eV. Values in parentheses are the estimated standard deviations obtained from the diagonal elements of the covariance matrix. The fit error is defined as $[\Sigma(\chi_{exp} - \chi_{calcd})^2 k^6 / \Sigma(\chi_{exp})^2 k^6]^{1/2}$.

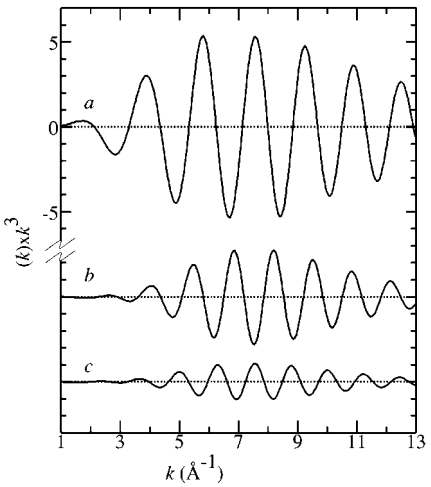

FIGURE 4: Individual contributions to the EXAFS of the best fit to the CuAce1 data of Figure 4. (a) First-shell EXAFS from three Cu−S ligands at 2.25 Å. Cu···Cu EXAFS from two atoms at 2.7 (b) and one at 2.9 Å (c). EXAFS for the two different Cu···Cu vectors are almost 180° out of phase, causing near cancellation of the longer interaction.

All the protein data sets yielded a small outer-shell transform peak at about 3.7 Å (Figure 5, arrow), which is also observed for $[Cu_4(SPh)_6]^{2-}$ (Figure 6, arrow). Simulation of the EXAFS of $[Cu_4(SPh)_6]^{2-}$, using the atomic coordinates from the crystallographically determined structure (*32*), indicates that the 3.7 Å feature arises from a combination of single scattering and multiple scattering paths involving distant copper and sulfur atoms within the cluster. Predominant among these are single scattering to the outer-shell sulfurs and (approximately equilateral) triangular multiple scattering paths involving three coppers. The small 3.7 Å protein peak can be modeled using the scattering paths

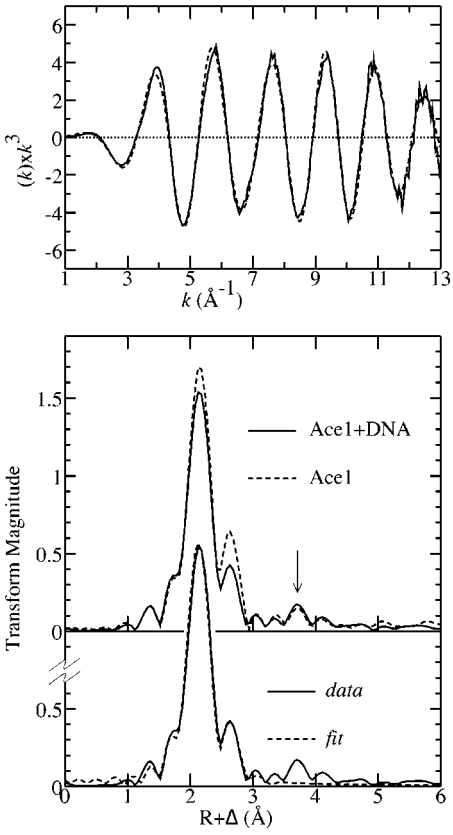

FIGURE 5: EXAFS of the CuAce1/DNA complex. The upper plot shows the EXAFS oscillations (solid line) and best fit (broken line), and the lower plot shows the experimental EXAFS Fourier transforms (Cu−S phase-corrected) of CuAce1 with and without DNA, and the best fit to the Ace1 + DNA data (bottom panel).

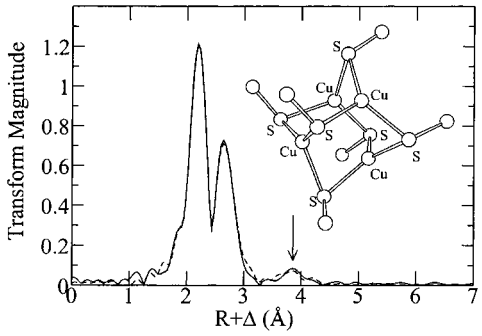

FIGURE 6: Long-range EXAFS in $[Cu_4(SPh)_6]^{2-}$. The figure shows the Cu−S phase-corrected Fourier transforms of the experimental EXAFS (solid line) and of the computed EXAFS (broken line) based on the crystal structure coordinates (see text). The long-range feature discussed in the text is indicated in the figure by the arrow, and the inset shows the polycopper core of the crystal structure.

calculated for $[Cu_4(SPh)_6]^{2-}$, with a slight adjustment in interatomic distances and Debye−Waller factors, and using a path degeneracy that suggests a tetranuclear cluster. A representative fit is shown for the CuAce1/DNA data set in Figure 7. These triangular Cu···Cu···Cu multiple scattering paths will be insensitive to the symmetrical cluster distortions discussed above, as the total path-length will always be the sum of one long and two short Cu···Cu vectors for the CuAce1 or for all three Cu···Cu vectors for CuAce1/DNA, which may account for the similar 3.7 Å peak intensities in the $[Cu_4(SPh)_6]^{2-}$ model and protein data sets. Thus, although it is the smallest resolved backscattering feature, the observation of the long-distance 3.7 Å interaction in the protein data

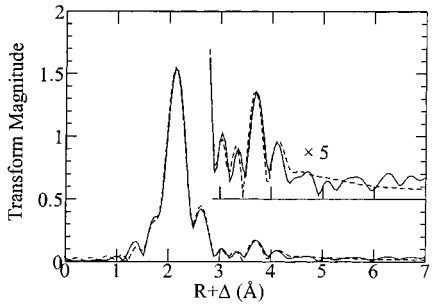

FIGURE 7: Example of curve-fitting analysis of the 3.7 Å feature. The EXAFS Fourier transform of the data (solid line) and best fit (broken line) to the CuAce1/DNA data is shown, with the high-R part vertically expanded (inset).

sets suggests the presence of $[Cu_4(SR)_6]^{2-}$ clusters in these samples and independently supports the results from fitting the 2.7 Å Cu···Cu backscattering.

DISCUSSION

X-ray absorption spectroscopy reveals the presence of remarkably similar polycopper clusters in both of the Cu-regulated transcription factors of *S. cerevisiae* (Ace1 and Mac1). In both, intense Cu−S backscattering, with a weaker Cu···Cu interaction apparently diminished by partial cancellation, dominates the EXAFS, and each cuprous ion possesses an approximately trigonal planar geometry. Both Ace1 and Mac1 bind 4 Cu(I) ions in their Cu-regulatory domains, although in Mac1 there are two repeats of the domain. Given that Ace1 is Cu-activated and Mac1 is Cu-inhibited, it is curious that structurally related polycopper clusters form in both proteins. One notable difference is that the cluster in Ace1 is more shielded from solvent, as indicated by the more prominent luminescence of CuAce1 compared to CuMac1(C1).

The ligands for both CuAce1 and CuMac1(C1) are predominantly cysteinyl thiolates. Eight cysteines are present within the 60 residue, Cu-regulatory domain of Ace1. In contrast, the C1 Cu-regulatory domain of Mac1 contains only five cysteines plus a conserved histidine. While only six of the eight cysteines in Ace1 are needed to explain the EXAFS results, we cannot exclude the possibility that all eight cysteines are involved in the cluster (i.e., not all thiolates in the cluster may be bridging). Mutational analysis reveals that all 8 cysteines in the Cu-regulatory domain are essential for Ace1 function (*45*). A search of the Cambridge Structural Database (*46*) for polycopper species containing the $Cu(SR)_3$ motif indicates that differences between bridging and nonbridging Cu−S bond-lengths are too small to be discerned by our EXAFS analysis, and we are thus unable to determine from this whether all thiolates in the Ace1 cluster are bridging. There are several examples of Cu_4S_8 clusters with an approximately tetrahedral tetracopper core similar to Cu_4S_6 but with two of the Cu−SR−Cu bridges replaced by nonbridging sulfur ligands to form a Cu_4S_8 cluster. Although a Cu_4S_8 is the candidate center in CuAce1, all Cu_4S_8 clusters in the Cambridge Structural Database have ligands in which considerable electron delocalization is expected such as thioacetate or thioamides. Density Functional Calculations of Cu_4S_8 clusters (not shown) using $R-S^-$ ligands indicate that such clusters may be unstable due to an excess of negative charge. The inherent instability of a Cu_4S_8 cluster in Ace1 may be an important feature in the transient Cu-activation of gene expression through Ace1.

The five conserved Cys residues and the single conserved His in the regulatory C1 motif in Mac1 are functionally important for Cu-regulation of Mac1 function (*14*). Thus, we might expect that a $Cu_4(S-Cys)_5(N-His)_1$ cluster forms in CuMac1(C1). If the C1 cluster contains a bridging imidazole nitrogen, two of the four copper atoms would have a single Cu−N bond, contributing nitrogen backscattering to the total EXAFS, with a coordination number of 0.5. Curve-fitting using 0.5 nitrogen and 2.5 sulfur ligands gave essentially indistinguishable fits to those using 3 sulfur ligands (Table 1), with the Cu−N EXAFS constituting only about 5% of the total EXAFS. Outer-shell carbon and nitrogen EXAFS are expected for histidine coordination and typically give rise to transform peaks at between ∼3 and 4 Å. Assuming a reasonable geometry for a bridging histidine (see below), we estimate that only the 3 Å peak would be significant. The contribution of this will be about 1% of the total EXAFS and close enough to the Cu···Cu EXAFS to be unobservable. We conclude that EXAFS lacks the sensitivity to detect a single nitrogen ligand in the copper cluster. Several low-molecular weight polycopper species with bridging nitrogen ligands are known (*47*, *48*). None of these compounds possesses an imidazole as a bridging ligand, and all are digonal cuprous species; however, related nitrogen-bridged complexes with trigonal Zn(II) (*49*) and a Ag(I) complex with bridging imidazole rings have been reported (*50*). Thus, a $Cu_4(S-Cys)_5(N-His)_1$ cluster with a histidine-derived nitrogen in place of a thiolate in a $[Cu_4(SR)_6]^{2-}$-like cluster is the likely copper center in the C1 motif of Mac1. Figure 8 shows plausible structures for the active sites of Mac1 and Ace1; both are refined coordinates using DFT, with hydrogen atoms on the external carbons (not shown). Our calculations predict that the $Cu_4SR_5N(His)$ cluster should be a stable structure and is thus a plausible candidate for the Mac1 cluster.

An alternative model, in which the copper is bound at two discrete binuclear sites, can be considered for Ace1. In this model, each binuclear copper site would possess two bridging cysteinyl thiolates and two external thiolates, thus requiring all eight cysteines to bind the four coppers. Each copper would be trigonally coordinated to cysteinyl sulfur with a Cu···Cu coordination number of one. This model cannot explain the copper coordination in Mac1 as only five cysteines are present for coordinating copper. A search of the Cambridge Structural Database reveals that such structures are unknown for Cu and Ag but are found for Zn and a few other transition metal ions. Typically, the metal−metal contact is longer than that observed for Ace1; for example, a distance of 3.5 Å is found in binuclear Zn compounds (*51*, *52*). Several examples of similar binuclear species with four-coordinate copper with all sulfur coordination to the metals are known (*53*), but these both require more sulfur ligands than are present and are in direct contradiction of our finding of three-coordinate copper in Mac1 and Ace1. Thus, we consider this model an unlikely candidate due to its chemical novelty, because of the similarity of Mac1 and Ace1 (the binuclear model can only occur in the latter), and finally because of the small 3.7 Å interaction, which we have discussed.

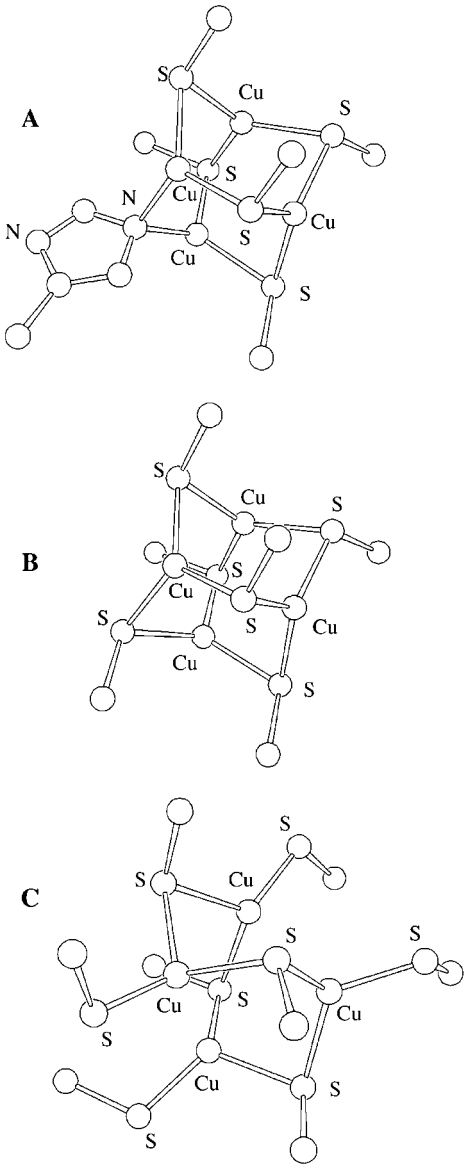

FIGURE 8: Postulated structures for the metal binding sites of Mac1 (A), a Cu_4S_6 cluster in Ace1 if Ace1 uses only six thiolates (B) or if the polycopper cluster in Ace1 has eight thiolates, four of which are nonbridging Cys.

Copper metalloregulation of Mac1 function correlates with the binding of Cu(I) within the C1 motif. The prediction is that polycopper cluster formation in C1 initiates the conformational switch that favors an intramolecular interaction between the N-terminal DNA binding domain and the C-terminal polycopper domain. Cu(I) binding to the C1 motif is abrogated in $Mac1^{up1}$ (*13*). Since the C2 domain contains a similar Cys-rich repeat, a polycopper cluster likely forms in this domain as well. It is unclear if or how metalation of the C2 motif modulates Mac1 function. The polycopper clusters formed within the repressed conformer of Mac1 are expected to form in an all-or-nothing manner analogous to the cooperative polycopper cluster formation in CuCup1 and CuAmt1 (*28*).

A curious observation in the present study is the attenuation of the Cu−Cu scatter peak when an oligonucleotide containing the Ace1 site is added to CuAce1. The change in EXAFS is suggestive of a DNA-induced distortion in the Ace1 tetracopper cluster. If the distortion destabilizes the copper cluster, DNA binding may be part of the mechanism of returning Ace1 to the silent state. In addition, the high charge density of a Cu_4S_8 cluster may also destabilize the Cu cluster.

The significance of a tetracopper cluster as the structural unit within Ace1 and Mac1 transcription factors is 3-fold. First, a polycopper cluster formed by up to eight cysteinyl residues in Ace1 and probably five cysteinyl and one histidine ligands in Mac1(C1) organizes and stabilizes a larger structural unit than a single bound metal ion. A single Cu(I) site is expected to be two-, three-, or possibly four-coordinate and, therefore, would anchor the polypeptide in at most three or four places rather than the six to eight anchor sites in the candidate copper-regulatory domain of Mac1 or Ace1.

A second significant aspect of a tetracopper cluster is that a polycopper cluster provides metal ion specificity. Ace1 is activated by either Cu(I) or Ag(I) but not by other metal ions (*15*, *54*). Polymetal−thiolate clusters are also known for Zn(II) and Cd(II), but these clusters are structurally distinct from the polycopper clusters (*55*). Cu(I) and Ag(I) polymetal−thiolate clusters contain metal ions with either digonal or trigonal coordination, whereas Zn(II) and Cd(II) polymetal−thiolate clusters are characterized by tetrahedral metal coordination (*55*), although in both cases, bridging thiolates are key features of cluster stability. Moreover, mammalian metallothionein isoforms 1 and 2 consist of two polymetal−thiolate clusters that are distinct depending on whether Zn(II) or Cu(I) ions are bound (*56*); the distinct clusters translate into metal-dependent structures. The observed activation of Ace1 by Cu(I) and Ag(I) is expected, since isostructural metal−thiolate cage clusters exist (*57*) (e.g., $[Cu_5(SPh)_7]^{2-}$ and $[Ag_5(SPh)_7]^{2-}$). Subtle structural differences observed between AgAce1 and CuAce1 (*24*) may relate to volume differences of the metal−thiolate cages for the two monovalent ions, since the mean Cu−S bond distance for a trigonally bound Cu(I) ion is 2.27 Å, compared with 2.50 Å for Ag−S (*57*). Cluster volume was implicated as a critical factor in metal ion binding within clusters in metallothionein (*58*). Thus, volume constraints as well as cluster geometry may be important factors in dictating metal ion specificity in Ace1 and Amt1.

The third important feature is the observed cooperativity in cluster formation. The tetracopper center in Amt1 was shown to form in an all-or-nothing manner (*28*). Cooperativity in Cu(I) binding was also reported for Ace1 in Cu(I) titration studies (*59*). Cooperativity in cluster formation may be significant in that it permits a direct coupling of the intracellular, exchangeable Cu ion concentration to transcriptional activation by CuAce1 and inhibition of transcription by metalation of Mac1. Cooperative cluster formation may yield a graded response in Ace1 and Mac1 function with respect to the cellular copper status. The extent of Mac1 inhibition or Ace1 activation may correlate with the Cu(I) concentration ferried to the nucleus by a putative metallochaperone.

REFERENCES

1. Jungmann, J., Reins, H. A., Lee, J., Romeo, A., Hassett, R., Kosman, D., and Jentsch, S. (1993) *EMBO J. 12*, 5051−5056.
2. Labbe, S., Zhu, Z., and Thiele, D. J. (1997) *J. Biol. Chem. 272*, 15951−15958.

3. Yamaguchi Iwai, Y., Serpe, M., Haile, D., Yang, W., Kosman, D. J., Klausner, R. D., and Dancis, A. (1997) *J. Biol. Chem. 272*, 17711−17718.
4. Hassett, R., and Kosman, D. J. (1995) *J. Biol. Chem. 270*, 128−134.
5. Georgatsou, E., Mavrogiananis, L. A., Fragiadakis, G. S., and Alexandraki, D. (1997) *J. Biol. Chem. 272*, 13786−13792.
6. Jensen, L. T., Posewitz, M. C., Srinivasan, C., and Winge, D. R. (1998) *J. Biol. Chem. 273*, 23805−23811.
7. Thiele, D. J. (1988) *Mol. Cell. Biol. 8*, 2745−2752.
8. Welch, J., Fogel, S., Buchman, C., and Karin, M. (1989) *EMBO J. 8*, 255−260.
9. Turner, R. B., Smith, D. L., Zawrotny, M. E., Summers, M. F., Posewitz, M. C., and Winge, D. R. (1998) *Nat. Struct. Biol. 5*, 551−555.
10. Jamison McDaniels, C. P., Jensen, L. T., Srinivasan, C., Winge, D. R., and Tullius, T. D. (1999) *J. Biol. Chem. 274*, 26962−26967.
11. Graden, J. A., and Winge, D. R. (1997) *Proc. Natl. Acad. Sci. U.S.A. 94*, 5550−5555.
12. Zhu, Z., Labbe, S., Pena, M. M. O., and Thiele, D. J. (1998) *J. Biol. Chem. 273*, 1277−1280.
13. Jensen, L. T., and Winge, D. R. (1998) *EMBO J. 17*, 5400−5408.
14. Keller, G., Gross, C., Kelleher, M., and Winge, D. R. (2000) *J. Biol. Chem. 275*, 29193−29199.
15. Furst, P., Hu, S., Hackett, R., and Hamer, D. (1988) *Cell 55*, 705−717.
16. Gralla, E. B., Thiele, D. J., Silar, P., and Valentine, J. S. (1991) *Proc. Natl. Acad. Sci. U.S.A. 88*, 8558−8562.
17. Culotta, V. C., Howard, W. R., and Liu, X. F. (1994) *J. Biol. Chem. 269*, 1−8.
18. Jensen, L. T., Howard, W. R., Strain, J. J., Winge, D. R., and Culotta, V. C. (1996) *J. Biol. Chem. 271*, 18514−18519.
19. Culotta, V. C., Joh, H. D., Lin, S. J., Slekar, K. H., and Strain, J. (1995) *J. Biol. Chem. 270*, 29991−29997.
20. Fogel, S., and Welch, J. W. (1982) *Proc. Natl. Acad. Sci. U.S.A. 79*, 5342−5346.
21. Hamer, D. H., Thiele, D. J., and Lemontt, J. E. (1985) *Science 228*, 685−690.
22. Ecker, D. J., Butt, T. R., Sternberg, E. J., Neeper, M. P., Debouck, C., Gorman, J. A., and Crooke, S. T. (1986) *J. Biol. Chem. 261*, 16895−16900.
23. Narula, S. S., Mehra, R. K., Winge, D. R., and Armitage, I. M. (1991) *J. Am. Chem. Soc. 113*, 9354−9358.
24. Peterson, C. W., Narula, S. S., and Armitage, I. M. (1996) *FEBS Lett. 379*, 85−93.
25. Rae, R. D., Schmidt, P. J., Pufahl, R. A., Culotta, V. C., and O'Halloran, T. V. (1999) *Science 284*, 805−807.
26. Farrell, R. A., Thorvaldsen, J. L., and Winge, D. R. (1996) *Biochemistry 35*, 1571−1580.
27. Graden, J. A., Posewitz, M. C., Simon, J. R., George, G. N., Pickering, I. J., and Winge, D. R. (1996) *Biochemistry 35*, 14583−14589.
28. Thorvaldsen, J. L., Sewell, A. K., Tanner, A. M., Peltier, J. M., Pickering, I. J., George, G. N., and Winge, D. R. (1994) *Biochemistry 33*, 9566−9577.
29. Pickering, I. J., George, G. N., Dameron, C. T., Kurz, B., Winge, D. R., and Dance, I. G. (1993) *J. Am. Chem. Soc. 115*, 9498−9505.
30. Rehr, J. J., Mustre de Leon, J., Zabinsky, S. I., and Albers, R. C. (1991) *J. Am. Chem. Soc. 113*, 5135−5140.
31. Mustre de Leon, J., Rehr, J. J., Zabinsky, S. I., and Albers, R. C. (1991) *Phys. Rev. 44*, 4146−4156.
32. Dance, I. G., Bowmaker, G. A., Clark, G. R., and Seadon, J. K. (1983) *Polyhedron 2*, 1031−1043
33. Koch, S. A., Fikar, R., Millar, M., and O'Sullivan, T. (1984) *Inorg. Chem. 23*, 121−122.
34. Delley, B. (1990) *J. Chem. Phys. 92*, 508−517.
35. Delley, B. (2000) *J. Chem. Phys. 113*, 7756−7764.
36. Becke, A. D. (1988) *J. Chem. Phys. 88*, 2547−2553.
37. Perdew, J. P.; Wang, Y. (1992) *Phys. Rev. B 45*, 13244−13249.
38. Ziegler, T. (1991) *Chem. Rev. 91*, 651−667.
39. Fan, L. and Ziegler, T. (1995) In *Density Functional Theory of Molecules, Clusters and Solids* (Ellis, D. E., Ed.) pp 67−95, Kluwer, Dordrecht, The Netherlands.
40. Scheiner, A. C., Baker, J., and Andzelm, J. W. (1997) *J. Comput. Chem. 18*, 775−795.
41. Curtiss, L. A., Raghavachari, K., Redfern, P. C., Pople, J. A. (1997) *J. Chem. Phys. 106*, 1063−1079.
42. Delley, B. (1995) In *Modern Density Functional Theory: A Tool for Chemistry* (Seminario, J. M., Politzer, P., Eds.) Vol. 2, pp 221−254, Elsevier, Amsterdam.
43. Kau, L.-S., Spira-Solomon, D. J., Penner-Hahn, J. E., Hodgson, K. O., and Solomon, E. I. (1987) *J. Am. Chem. Soc. 109*, 6433−6442.
44. Pufahl, R. A., Singer, C. P., Peariso, K. L., Lin, S.-J., Schmidt, P., Fahrni, C., Culotta, V. C., Penner-Hahn, J. E., and O'Halloran, T. V. O. (1997) *Science 278*, 853−856
45. Hu, S., Furst, P., and Hamer, D. (1990) *New Biologist 2*, 544−555
46. Allen, F. H. and Kennard, O. (1993) *Chem. Des. Autom. News 1*, 31−37.
47. Gambarotta, S., Bracci, M., Floriani, C., Chiesi-Villa, A. and Guastini, C. (1987) *J. Chem. Soc., Dalton Trans.* 1883−1888.
48. Hope, H. and Power, P. P. (1984) *Inorg. Chem. 23*, 936−937.
49. Putzer, M. A., Dashti-Mommertz, A., Neumuller, B., and Dehnicke, K. (1999) *Z. Anorg. Allg. Chem. 624*, 263−266.
50. Hintermaier, F., Mihan, S., Gerdan, M., Schunemann, V., Trautwein, A., and Beck, W. (1996) *Chem. Ber. 129*, 571−573.
51. Grutzmacher, H., Steiner, M., Pritzkow, H., Zsolnai, L., Huttner, G., and Sebald, A. (1992) *Chem. Ber. 125*, 2199−2213.
52. Bochmann, M., Bwembya, G., Grinter, R., Lu, J., Webb, K. J., Williamson, D. J., Hursthouse, M. B., Mazid, M. (1993) *Inorg. Chem. 32*, 532−537.
53. Davies, S. C., Durrant, M. C, Hughes, D. L., Leidenberger, K., Stapper, C., and Richards, R. L. (1997) *J. Chem. Soc., Dalton Trans. (14)*, 2409−2418.
54. Dameron, C. T., Winge, D. R., George, G. N., Sansone, M., Hu, S., and Hamer, D. (1991) *Proc. Natl. Acad. Sci. U.S.A. 88*, 6127−6131.
55. Dance, I. G. (1986) *Polyhedron 5*, 1037−1104.
56. Winge, D. R., Dameron, C. T., and George, G. N. (1994) *Adv. Inorg. Biochem. 10*, 1−48.
57. Dance, I. G. (1978) *Aust. J. Chem. 31*, 2195−2206.
58. Good, M., Hollenstein, R., and Vasak, M. (1991) *Eur. J. Biochem. 197*, 655−659.
59. Casas-Finet, J. R., Hu, S., Hamer, D., and Karpel, R. L. (1992) *Biochemistry 31*, 6617−6626.

BI0160664